Mineralogical characteristics of sulfuric acid formation during bacterial oxidation of flotation concentrate

Sanat Sharipov*, *Bakhodir* Mukhiddinov, *Fakhriyor* Oliqulov, and *Jurabek* Shodikulov

Navoi State University of Mining and Technologies, Navoi, 210100, Uzbekistan

Abstract. The article presents the results of a study on the formation of sulfuric acid in the process of bacterial oxidation of sulfide ore flotation concentrate. The results are estimated from the point of view of the thermodynamics of the course of some bacterial oxidation reactions, calculating the standard enthalpies of formation - (ΔH^0_{298}), entropy (ΔS^0_{298}) and Gibbs energy of formation (ΔG^0_{298}) of some reactions and substances at 298 K. Conclusions about the formation of sulfuric acid based on X-ray phase and electron scanning microscope results of changes in mineralogical and elemental composition in the processes of bacterial oxidation of flotation concentrate are substantiated.

1 Introduction

In present time the world's reserves of deposits with high initial content and easily recoverable ores are practically depleted and at the same time the share of gold is increasing in primaryh rudah, related to the category of persistent gold-bearing mineral raw materials. These minerals consist ofIt mainly from pyrite, arsenopyrite, chalcopyrite, hydroarsenatebut iron, oxidebut manganese and othersh [1-2].

Microorganisms are an important evolutionary link that catalyzes the appearance of new mineral compounds and accelerates their formation. As is known, biochemical reactions occurring during the biological oxidation of sulfide minerals can occur either by a direct or indirect mechanism [3]. The direct mechanism requires close physical contact between the bacteria and the mineral surface to ensure that the bacteria attach to the mineral, while the indirect mechanism involves the action of bacterial-generated iron sulfate (III). Iron ions are mainly found in the composition of ore minerals-pyrite (FeS_2) and arsenopyrite (FeAsS), also as part of the fayalita ($Fe_2[SiCl_4]$) [1,4].

Iron atoms in the composition of sulfide minerals are in divalent form [5]. During bacterial leaching in sulfuric acid oxidation reactors, they pass into solution in the form of ferrous and trivalent iron sulfates. In the process of bacterial leaching, pyrite sulfide sulfur is oxidized to sulfate, and nitrous ironabout up to the oxide level and two products are formed; iron sulfate and sulfuric acid.

* Corresponding author: element_2993@mail.ru

© The Authors, published by EDP Sciences. This is an open access article distributed under the terms of the Creative Commons Attribution License 4.0 (https://creativecommons.org/licenses/by/4.0/).

Iron sulphate chemically oxidizes pyrite and arsenopyrite, having formed nitrous iron sulfate and elementaryuyu serat. Nitrous iron is again oxidized by bacteria to oxide, which can be consumed as an oxidizer of pyrite and arsenopyrite.

The leading role in the implementation of these transformations belongs to the thion bacteria T. ferrooxidans, which oxidizes sulfides and nitrous iron, T. thiooxidanya, which oxidizes elemental sulfur.

Aboutabsence of thion bacteria - oxidizing agents of minerals can in principle serve as oxygen dissolved in the form ofbut and sulfuric acidgo окисногo iron [6-8].

Bacterial oxidation of persistent gold-bearing ores mainly occurs intensively at pH=1.2-1.4 and at a temperature of 303-316 K.

This raises a question. Due to the dissolution of what ore mineral is a highly acidic environment formed?

To clarify this issue, please contact us The mineralogical composition of the solid part of the bacterial oxidation process was studied, including changes in the pyrite concentration (FeS_2), arsenopyrite (FeAsS), stibnite (Sb_2S_3), jarosite ($MFe_3(SO_4)_2(OH)_6$, by modern physico-chemical methods of analysis.

2 Materials and methods

Samples were taken from an experimental reactor with a volume of 50 liters. 34 liters of inoculum from the BIOX module No. 1 with a pH of 1.32 and a density of 1100 g/l were used to start the reactor.

Flotation concentrate was brought from the UPS (raw material preparation unit) in the amount of 20 liters, with a density of 1335 g / l, the content of total sulfur-17.8 %, sulfide sulfur-14.13 %, total carbon-2.47 %, organic carbon-1.34 (sample No. 793).

The inoculum was poured into the reactor and 1 liter of flotation concentrate was supplied every 2 hours. After starting the reactor, samples were taken based on the pH of the medium:flotation concentrate pH-8.2 sample No. 793; biokek pH-1.39 sample 842; biokek pH-1.42 sample 843; biokek pH-1.37 sample 869; biokek 1.40 sample 870; biokek pH-1.34 sample 917.

Henceforth, all tabular and graphic materials will refer to samples by their names.

The diffractograms were obtained on a powder X-ray diffractometer of the brand "Shimadzu XRD-6100", equipped with a copper (Cu) by phone (K ∞1=1,5406Å, To ∞2 = 1,5443, To∞2 / K ∞1=0,5. The detector is a scintillation detector. A scanning electron microscope was used (Carl Zeiss, Germany) with an energy-dispersion element analyzer (Oxford Instruments, United Kingdom).

3 Results

Bacterial attack of arsenopyrite and pyrite occurs mainly through a direct contact mechanism. The equations for the oxidation reactions of pyrite and arsenopyrite are given below (see reactions 1-9 and 12-20):

$$4FeAsS+13O_2+6H_2O \xrightarrow{bacteria} 4H_3AsO_4+4FeSO_4 \quad (1)$$

$$4FeAsS+11O_2+6H_2O \xrightarrow{bacteria} 4H_3AsO_3+4FeSO_4 \quad (2)$$

$$H_3AsO_3 + Fe_2(SO_4)_3 +H_2O \xrightarrow{chemically} 2FeSO_4+H_3AsO_4+ H_2SO_4 \quad (3)$$

$$2S+3O_2+2H_2O \xrightarrow{bacteria} 2H_2SO_4 \quad (4)$$

$$4FeS_2+15O_2+2H_2O \xrightarrow{bacteria} 2Fe_2(SO_4)_3+2H_2SO_4 \quad (5)$$

$$FeS_2+Fe_2(SO_4)_3 \xrightarrow{chemically} 3FeSO_4+2S \quad (6)$$

$$4FeSO_4 + O_2 + 2H_2SO_4 \xrightarrow{bacteria} 2Fe_2(SO_4)_3 + 2H_2O \quad (7)$$

$$2FeAsS + 2Fe_2(SO_4)_3 + 2H_2O + \frac{5}{2}O_2 \rightarrow 2H_3AsO_4 + 6FeSO_4 + 2S \quad (8)$$

$$2FeAsS + 2Fe_2(SO_4)_3 + 5H_2O + \frac{11}{2}O_2 \rightarrow 2H_3AsO_4 + 6FeSO_4 + 2H_2SO_4 \quad (9)$$

Next, the reactions (4) and (7) are repeated, forming $Fe_2(SO_4)_3$ and H_2SO_4.

Some bacterial oxidation reactions can be characterized in terms of thermodynamics. The enthalpy of formation, entropy of formation, and Gibbs energy of the reaction were calculated using the following formulas:

$$\Delta H^0_{reac} = \sum \Delta H^0_{298b} - \sum \Delta H^0_{298a}$$

Standardth enthalpy of formation ΔH^0_{298}, entropy ΔS^0_{298} and Gibbs energy ΔG^0_{298} a certain personsubstances at 298 K (Table 1).

Table 1. Thermodynamic characteristics of some substances involved in bacterial oxidation processes.

Substance	Physical condition	Enthalpy, KJ/mol	Entropy, J/mol*K	Free energy (Gibbs), Kj/mol
FeS_2	Crystal	-177.40(-163.2)	52.99	-266.05
$FeSO_4$	Crystal	-927.59(-3016)	107.53	-819.77
FeS	Crystal	-100.42	60.29	-200.75
H_2O	Liquid	-295.83	69,65	-237.23
H_2SO_4	Liquid	-813.99	156.90	-290.14
$Na_2S_2O_3$	Crystal	-1117.73	255	-2043
S	Solid	0	32.55	0
SO_2	Gas	-296.95	248.67	-300.27
SO_3	Gas	-395.85	256.69	-317.27
CuS	crystal	-53.14	66.53	-53.58
H_2S	Gas	-20.60	205.70	-33.50
$Fe_2(SO_4)_3$	Crystal	-2584	282.9	-2253
Ar_2O_5	Crystal	-924.9	59.5	-782.4
Ar_2S_3	Crystal	-159	163.6	-158
Ar_2O_3	Crystal	-1334.7	233.5	-1176.4
Ar	Solid	-	36.6	0
O_2	Gas	0	205.0	-

$$\Delta S^0_{298} = \sum \Delta S^0_{298} - \sum \Delta S^0_{298} \quad (10)$$

$$\Delta G = \Delta H - T\Delta S \quad (11)$$

Calculation results ΔH_{reac}, ΔS_{reac} and ΔG_{reac} for some bacterial oxidation reactions, pyrite and arsenopyrite are shown in Table 2.

Table 2. Basic thermodynamic parameters ΔH_{reac}, ΔS_{reac} and ΔG_{reac} for the process of bacterial oxidation of flotation concentrate.

Numbering reactions	$\Delta H_{reac.}$, kJ/mol	$\Delta S_{reac.}$, $J \cdot K^{-1}$	$\Delta G_{reac.}$, kJ/mol	Note
1	-2928.5	-245.6	-76164.5	$\Delta G<0$
2	-6296	-956.7	-291392.6	$\Delta G<0$
3	-7139	-1293.1	378324	$\Delta G>0$

4	-1056.34	-505.4	149552.9	ΔG>0
5	-	-	-230.6	ΔG<0(293K)
6	-	-	-	-
7	-	-	-	-
8	-	-	-4319.5	ΔG<0 (293K)
9	-	-	-4592.2	ΔG<0(293K)

$\Delta G\text{reac} < 0$ - the reaction under these conditions proceeds spontaneously
$\Delta\Delta G > 0 -$ the reaction does not occur spontaneously (Table 2) [9].

Analysis of the study results (Table 2) shows that the numerical value of the Gibbs energy of the formation ΔG^0_{298} arsenopyrite dissolution reactions (No. 9) are less than pyrite dissolution reactions (No. 5). This indicates that the arsenopyrite dissolution reaction proceeds more easily than the pyrite dissolution reaction. These results are also consistent with the results of X-ray phase and scanning electron microscopy.

According to some data, intermediate products of sulfide oxidation (thiosulfate ($H_2S_2O_3$), possibly polythionates) formed with the participation of T. ferrooxsidans and T. Denifrificans and other thion bacteria can form water-soluble complexes of thiosulfate ions, according to stroPlease note: close to sulfate ions. In the tetrahedron $[SO_3S]^{2-}$ S-S connection (1.97 Å) is longer than the S-O bonds (1.48 Å)

Iron ions (III) can break the chemical bond in the lattice between iron and disulfide after the disulfide group is oxidized to thiosulfate. According to the "thiosulfate" mechanism, pyrite and arsenopyrite are exposed to an iron hexahydrate ion (III), as a result, the first intermediate product of oxidation is the thiosulfate ion, in the next step, the thiosulfate is oxidized Fe^{3+} - ions to tetrathionate, which hydrolyzes to form a sulfate ion and disulfate monosulfonic acid ($R\text{-}SO_3RH$), and it is oxidized to threetionata, threetionate is hydrolyzed to sulfate and thiosulfate ions.

As by-products during the oxidation process, the formation of pentathionate and the elementapnoi sera. Chemical or bacterial oxidation of intermediates occurs with the participation of Fe^{3+} - ions or molecular oxygen (as an electron acceptor). Since thiosulfate is a key compound in the process of biooxidation of the sulfuric part of pyrite, this mechanism is interpreted as thiosulfate.

The reaction equation is given by below.

$$2FeS_2+18H_2O+12[Fe(H_2O)_6]\rightarrow 32H^++2S_2O_3^{2-}+14[Fe(H_2O)_6]^{2+} \quad (12)$$

$$2S_2O_3+H_2O\rightarrow H_2SO_4+S_3O_3^{2-} \quad (13)$$

$$2S_3O_3^{2-} + 3H_2O+3Fe_2(SO_4)_3\rightarrow 6FeSO_4+ 6H^++1{,}5O_2+3S_3O_6^- \quad (14)$$

$$S_3O_6^{2-} + H_2O\rightarrow 2H^+ + SO_4^{2-} + S_2O_3^{2-} \quad (15)$$

$$S_3O_3^{2-} + S_2O_3^{2-} + 2Fe^{3+} + (0{,}5O_2+2H^+) \rightarrow S_5O_6^{2-}+2Fe^{2+} + (H_2O) \quad (16)$$

$$S_3O_3^{2-} \rightarrow 0{,}25S_8 + SO_3^{2-} \quad (17)$$

$$SO_3^{2-} + 2Fe^{3+} +H_2O \rightarrow SO_4^{2-} + 2Fe^{2+} + 2H^+ \quad (18)$$

$$S_3O_3^{2-} + S_4O_6^{2-}\rightarrow S_2O_3^{2-} + S_5O_6^{2-} \quad (19)$$

$$MeS+2H^++Fe^{3+}\rightarrow Me^{2+}+Fe^{2+}+(H_2S^*)\rightarrow H^++HS^+\rightarrow H_2S_n^{+}+Fe^{3+}\rightarrow S_8+H^++Fe^{2+} \quad (20)$$

Also, to confirm the mechanism of sulfuric acid formation, the mineralogical and elemental composition of the solid part of the bacterial oxidation process was studied. Changes in pyrite concentrations (FeS_2), arsenopyrite (FeAsS), stibnite (Sb_2S_3), jarosite ($MFe_3(SO_4)_2(OH)_6$, where $Me=K^+$, Na^+or NH_4^+), yarosite hydronium $[(H_3O)Fe_3(SO_4)_2(OH)_6]$ and calcium sulfates were studied in detail using scanning electron microscopy methods c energy-dispersion detector for semi-quantitative elemental analysis and x-ray phase analysis.

Education Irosita ($MFe_3(SO_4)_2(OH)_6$) and yarosite hydronium $[(H_3O)Fe_3(SO_4)_2(OH)_6]$ at high temperatures concentrations of chloride ions (more than 5 g / l) it can lead to a decrease in gold recovery during cyanidation [10].

Samples from the experimental reactor were studied using the following methods: electron microscopy c energy-dispersion detector for semi-quantitative elemental analysis and x-ray phase analysis. Samples from the process chain were studied by X-ray phase analysis, the results of which are shown in Figure 1.

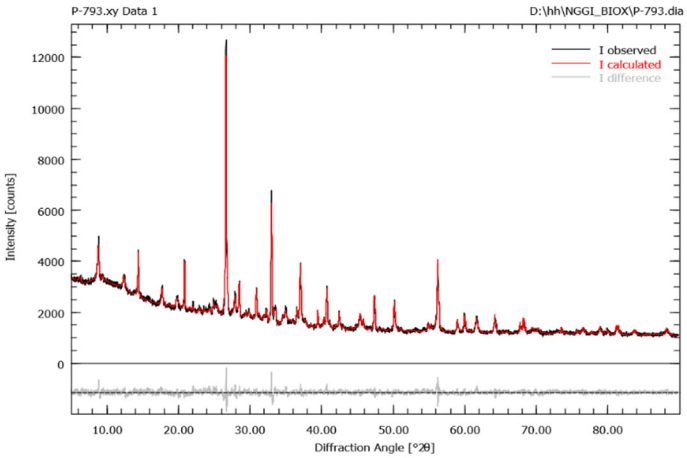

Fig. 1. X-ray image of a prototype reactor sample (flotation concentrate pH-8.2 sample No. 793).

X-ray phase analysis by the Rietveld method was performed using the Profex-Open sourse XRD and Reitveld Refinement software [9], the results of which are presented in Table 3.

Table 3. Semi-quantitative mineralogical composition of sample No. 793.

№	Mineral name	Chemical formula of the mineral	Content, (%)
1.	Pyrite	FeS_2	13.7
2.	Quartz	SiO_2	16.9
3.	Muscovite	$KAl_2(AlSi_3O_{10})(OH)_2$	30.2
4.	Clinochlore	$Mg_5Al(AlSi_3O_{10})(OH)_8$	0.85
5.	Calcite	$CaCO_3$	1.51
6.	Anorthitis	$CaO{\cdot}Al_2O_3{\cdot}2SiO_2$	11.4
7.	Arsenopyrite	FeAsS	3.27
8.	Monticellite	$CaMgSiO_4$	4.27
9.	Ankerit	$Ca(Mg, Fe)\ [CO_3]_2$	3.2
10.	Dickit	$Al_2[Si_2About_5]\ (HE)_4$	3.04
11.	Chlorit2b	$(Mg,Fe)_3(Si,Al)_4O_{10}(OH)_2{\cdot}(Mg, Fe)_3(OH)_6$	6.33
12.	Talcum powder	$Mg_3Si_4O_{10}(OH)_2$	1.27
13.	Graphite	With	4.05

Analysis of the study results (Table 3) shows that mine-ralogical composition of sample No. 793, mainly composed of pyrite (FeS_2) -13.7%, quartz (SiO_2) -16.9 %, muscovite ($KAl_2(AlSi_3O_{10})(OH)_2$) -30.2%, anorthite ($CaO{\cdot}Al_2O_3{\cdot}2SiO_2$) – 11.4%, arsenopyrite (FeAsS) - 3.27% and other components.

Other flotation concentrate samples were also examined by X-ray phase analysis: pH-8.2 sample No. 793; biokek pH-1.39 sample 842; biokek pH-1.42 sample 843; biokek pH-1.37 sample 869; biokek 1.40 sample 870; biokek pH-1.34 sample 917.

Diffractograms of the above samples processed also by the Rietveld method, generalized values the results of which are presented in Table 4.

Table 4. Summary mineralogical composition of selected solid samples №793, №842, №843, №869, №870 and #917.

№	Name mineral content	Samples					
		№793	№842	№843	№869	№870	№917
1	Pyrite	13.7	4.10	5.73	3.76	28.28	1.79
2	Quartz	16.9	31.32	30.93	28.26	28.28	28.07
3	Muscovite	30.2	40.65	42.06	40.47	33.74	45.07
4	Clinochlore	0.85	-	0.63	1.62	1.7	-
5	Anorthitis	11.4	7.89	10.44	10.4	12.82	10.68
6	Arsenopyrite	3.27	2.01	1.84	0.37	-	-
7	Dickit	3.04	1.06	0.81	1.72	1.11	0.44
8	Chlorit2b	6.33	2.45	1.9	2.57	2.52	2.48
9	Graphite	4.05	1.3	1.68	2.95	4.75	1.48
10	Gypsum	-	1.21	-	-	1.27	1.36
11	Rutile	-	0.98	-	0.58	-	-
12	Kaolin	-	0.75	-	1.11	2.54	1.14
13	Hydronium nitrite	-	0.243	0.25	-	0.73	0.32
14	Yarozit	-	3.74	3.28	4.16	3.24	3.12
15	Anataz	-	0.739	-	1,19	1.709	1.052
16	Nakrit	-	1.55	0.46	0.79	1.86	-
17	Molibdenite	-	-	-	-	0.062	0.031
18	Hydrotalcit	-	-	-	-	-	2.97
19	Calcite	1.51	-	-	-	-	-
20	Monticellite	4.27	-	-	-	-	-
21	Ankerit	3.2	-	-	-	-	-
22	Talcum powder	1.27	-	-	-	-	-

Table 4 presents the results of mineralogical analysis of solid samples numbered in the laboratory of GTI hydrometallurgical plant. The composition of minerals is quite diverse, represented mainly by transformations of rock-forming minerals. Indeed, the majority of microorganisms interacted with rock-forming, accessory, and ore minerals. While pyrite, arsenopyrite, muscovite, rutile, jarosite, and molybdite are ore minerals, the vast majority of minerals were rock – forming-quartz, feldspar, dickite, calcite, gypsum, ankerite, and others. In quantitative terms it is the rock-forming minerals that have been exposed to microorganisms. The most interesting aspect of the research was the maximum change in aluminosilicate minerals.

Analysis of the study results shows that the amount of pyrite varies in the samples from 13.7% to 1.79%, and arsenopyrite from 3.27% before 0.37%, and in samples No. 870 and No. 917 are missing.ov arsenopyrite. These results show that the formation of sulfuric acid, mostly, to the imageeIt is produced by arsenopyrite and pyrite.

The elemental composition of the selected solid samples was also determined using a scanning electron microscope№793, №842, №843, №869, №870 and No. 917, the results of which are presented below on Figure 2 and in Table 5.

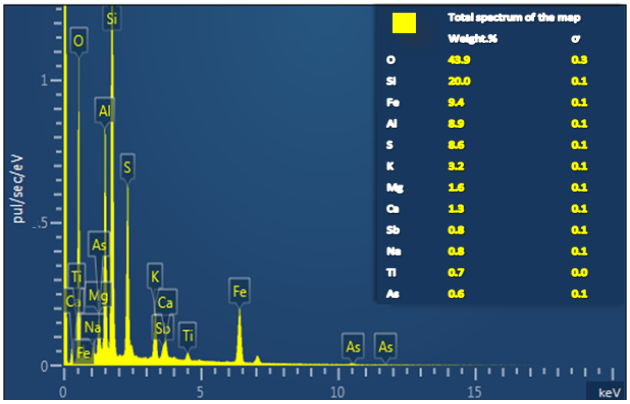

Fig. 2. Semi-quantitative elemental composition obtained from the surface of sample No. 793 and the corresponding energy-dispersion spectrum.

Analysis of the energy-dispersion spectrum (Figure 2) shows that sample No. 793 consists mainly of oxygen -43.9%, silicon-20.0%, and ironbut- 9.4%, aluminum-8.9%, sulfur -8.6, arsenic -0.6% and othersh elements.

Table 5. Summary of the elemental composition of selected solid samples №793, №842, №843, №869, №870 and No. 917 obtained by scanning electron microscope.

№ n/a	Name of elementbut	Numbering of samples					
		№ 793	№ 842	№ 843	№ 869	№ 870	№ 917
		weight, %	weight, %	weight, %	weight, %	weight, %	weight, %
1.	O	43.93	48.55	48.65	49.78	42.04	50.20
2.	Na	0.76	0.71	0.71	0.78	0.43	0.74
3.	Mg	1.64	1.28	1.27	1.40	0.86	1.30
4.	Al	8.89	10.41	10.40	10.85	6.74	10.60
5.	Si	19.96	23.20	23.49	24.06	14.15	23.85
6.	S	8.61	2.55	3.53	2.62	2.33	1.90
7.	K	3.24	3.63	4.00	3.99	2.64	4.08
8.	Ca	1.34	0.29	0.34	0.17	0.53	0.06
9.	Ti	0.74	0.82	0.84	0.86	0.52	0.85
10.	Fe	9.41	4.72	5.51	4.69	3.31	3.99
11.	As	0.64	0.64	0.61	0.49	0.16	0.16
12.	Sb	0.85	0.96	0.54	0.31	-	-
13.	In	-	1.51	-	-	-	-
14.	C	-	0.71	-	-	26.28	-
15.	P	-	-	0.11	-	-	-
16.	N	-	-	-	-	-	2.26
	The amount	100.00	100.00	100.00	100.00	100.00	100.00

4 Conclusion

Comparison of the elemental composition of selected solid samples №793, №842, №843, №869, №870 and №917, obtained with a scanning electron microscope, also confirms the

formation of sulfuric acid, mainly from arsenopyrite and pyrite. For example, the content ofe elementapThe sulfur content decreases from 8.61% to 1.90%, and the arsenic content decreases from 0.64% to 0.16%.

Thus, the formation of sulfuric acid in the process of bacterial oxidation of the flotation concentrate is justified by the fact that the mineral arsenopyrite undergoes oxidation at the beginning, and then pyrite and other sulfur-containing minerals are oxidized.

References

1. P. Valdivieso-Bermeo, I. Peñaloza, J. Moreno-Chávez, Treatment for gold ores with high content of carbonaceous matter DYNA **87(215)**, 180-185 (2020)
2. M.A. Meretukov, K.S. Sanakulov, A.V. Zimin, M.A. Arustamyan, *Gold: chemistry for metallurgists and concentrators* (Moscow, Ore and Metals Publishing House, 2014) 411
3. J. Hua, H. Huang, H. Xie, L. Gand, J. Liud, M. Long, Biochem. Eng. J. **128**, 228-234 (2017)
4. J. Ahna, J. Wua, J. Ahnb, J. Leea, Miner. Eng. **140**, 8 (2019)
5. J.J. Roy, M. Srinivasan, B. Cao, ACS Sustain. Chem. Eng. **9**, 3060-3069 (2021)
6. K.S. Sanakulov, B.F. Mukhiddinov, S.Sh. Sharipov, Kh.M. Vapoev, Tsvetnye Metally **5**, 15-23 (2022). https://www.doi.org/10.17580/tsm.2022.05.01
7. S.H. Andrianandraina, J. Dionne, H. Darvishi-Alamdari, J.F. Blais, Miner. Eng. **176**, 107360 (2022)
8. G.V. Sedelnikova, *Biogeotechnology of gold extraction from non-traditional mineral raw materials.* The dissertation author's abstract on competition of a scientific degree of the doctor of technical sciences 24 (1999)
9. E. Douglas, D. Rawlings, B. Johnson, *Biomining* (Springer, 2006)
10. N. Döbelin, R. Kleeberg, Journal of Applied Crystallography **48**, 1573-1580 (2015)